Journal of Materials, Processing and Design (2025)
Clausius Scientific Press, Canada

DOI: 10.23977/jmpd.2025.090104
ISSN 2516-0923 Vol. 9 Num. 1

Microstructural Evolution and Strengthening Mechanisms of 1100 Aluminum Foil under High Strain

Mingyuan Jiang[a], Qiuhong Pan[b,*], Xuan Li[c], Haoyang Cheng[d]

School of Materials Science and Engineering, Jiangsu University, Zhenjiang, China
[a]1245350421@qq.com, [b]panhong9004@163.com, [c]1176628939@qq.com, [d]953205762@qq.com
**Corresponding author*

Keywords: 1100 aluminum alloy, severe deformation rolling, grain morphology, mechanical properties

Abstract: This study systematically investigated the grain structure evolution of 1100 aluminum alloy during rolling processes and the strengthening mechanisms of 13 μm ultra-thin aluminum foil. Metallographic observations revealed that the as-cast rolled sheet exhibited fibrous grain structures, with refined edge grains and coarser central layer grains determined by temperature gradients induced by roller cooling. During cold rolling and foil rolling (6.8 mm → 13 μm), grains experienced severe elongation along the rolling direction, with thickness compressed from millimeter-scale to nano-scale (20-50 nm). This process formed lamellar nanocrystalline bands and periodic shear bands (200 nm spacing), accompanied by significantly increased dislocation density, ultimately creating fiber bundle structures with aspect ratios exceeding 40:1. Annealing experiments demonstrated that 460 ℃/3h treatment rapidly recrystallized fibrous grains into equiaxed grains. Transmission electron microscopy (TEM) analysis revealed high-density dislocation tangles, dislocation walls, and subgrains within 13 μm foil. Severe dislocation pile-ups at grain boundaries substantially impeded dislocation motion, elevating tensile strength to 250 MPa. Mechanical property analysis identified three synergistic strengthening mechanisms: 1) Dominant grain refinement strengthening; 2) Significant dislocation strengthening; 3) Second-phase strengthening. Their combined effects enabled the foil to achieve both high strength (250 MPa) and moderate ductility (3.5%), surpassing the theoretical strength limit of pure aluminum. This research provides theoretical guidance for process optimization of high-performance battery aluminum foils, demonstrating the critical role of multi-scale microstructure control in balancing material strength and toughness.

1. Introduction

Aluminum alloy materials are widely used in automotive, construction, and aerospace industries due to their comprehensive cost-performance advantages. To meet structural and functional requirements, many applications impose critical demands on non-heat-treatable aluminum alloys, including ultra-thin gauge, high strength-toughness combination, stable formability, as well as safety and durability requirements. As a crucial functional material, the processing techniques of aluminum foil directly determine its microstructural characteristics, mechanical properties, and surface quality.

The manufacturing of ultra-thin battery aluminum foil (typically <20 μm thickness) requires the integration of high-precision rolling technologies, microstructural control strategies, and surface quality management systems with conventional foil processing techniques. The production of aluminum foil primarily involves processes including melting and casting, hot rolling, cold rolling, foil rolling, and post-treatment. Three main production methods exist: deposition method, pack rolling method, and strip casting and rolling method. Currently, most manufacturers predominantly adopt the strip casting and rolling method due to its higher efficiency and lower cost compared to alternative approaches. This paper investigates the microstructural evolution of 1100 aluminum alloy during casting-rolling, cold rolling, and foil rolling processes, and explores the strengthening mechanisms of the final aluminum foil products. For non-heat-treatable aluminum alloys, the strengthening mechanisms primarily rely on strain hardening, solid solution strengthening, grain refinement, and second-phase particle strengthening. As strain hardening progresses to a certain extent, the enhancement in strength is inevitably accompanied by a reduction in plasticity. Numerous researchers have investigated this phenomenon. Niels Hansen[1] et al. systematically analyzed the interplay between microstructural evolution and local texture development in 1050 aluminum alloy under ultra-high strain conditions. Their[2] findings demonstrated that both the cold-rolled high-strain texture and post-annealing microstructure play critical roles in recovery and recrystallization processes, although the exact correlation mechanism remains undefined. Other researchers have employed severe plastic deformation (SPD) techniques such as accumulative roll bonding (ARB), equal-channel angular pressing (ECAP), and high-pressure torsion (HPT) to achieve grain refinement for enhancing the strength-toughness synergy in aluminum alloys. Studies by X. Huang et al. revealed that ARB processing induces unconventional microstructural evolution in commercial-purity aluminum during high-strain-rate deformation, primarily attributed to the introduction of shear strains that may alter the characteristic slip mechanisms of conventional rolling. When grain sizes are refined to specific dimensions (d >10-20 nm), nanomaterials exhibit a classic strength-plasticity trade-off: while strength increases with decreasing grain size, the limited dislocation storage capacity in nanograins results in significantly reduced ductility. Research[3,4,5] has demonstrated that incorporating nanoscale second-phase particles into nanocrystalline materials enables simultaneous enhancement of both strength and plasticity. Cheng et al. demonstrated that introducing nano-precipitates via a novel nanoprecipitation strategy effectively optimizes the strength-ductility synergy in 2024 aluminum alloy. Extensive studies confirm that the concurrent enhancement of yield strength and plasticity originates from second-phase strengthening. However, this approach remains challenging for non-heat-treatable aluminum alloys owing to the absence of precipitation-hardening phases. Previous research on these alloys has predominantly focused on deformation processing, intermediate annealing, and phase transformation of secondary phases, with limited in-depth exploration of their intrinsic strengthening-toughening mechanisms. Notably, 1100 aluminum alloy exhibits superior advantages in mechanical properties, surface quality, and ultra-thin gauge formability compared to other non-heat-treatable soft aluminum alloys, particularly achieving appreciable strength when foil-rolled to specific thicknesses. This study employs a conventional rolling route using cast-rolled slabs to fabricate aluminum foils under high-strain processing. We systematically investigate the correlation between strengthening-toughening mechanisms and refined grain structures (20-50 nm thickness) coupled with second-phase particle size distribution (5-15 nm) in 1xxx-series aluminum foils under severe deformation (total reduction >99.8%). The findings provide a viable pathway for attaining high strength-toughness combinations in non-age-hardenable aluminum alloys through microstructure engineering.

2. Materials and Experimental Procedures

The experimental material employed in this study was industrial 1100 aluminum alloy supplied by an aluminum manufacturing corporation, with chemical composition of 0.95Fe-0.95Si-0.20Cu-0.05Mn-balance Al (wt.%). The as-received material consisted of 6.8 mm thick cast-rolled sheets, which were subsequently processed through multi-pass rolling to achieve various thicknesses: 2.2 mm, 0.96 mm, 0.46 mm, 0.26 mm, 0.1 mm, 40 μm, and 13 μm, as schematically illustrated in Figure 1.

All foil samples underwent standardized metallographic preparation: initial rough grinding followed by mechanical polishing and subsequent electropolishing. Microstructural characterization was performed using optical microscopy and electron backscatter diffraction (EBSD) analysis conducted on a FEI NovaNano450-7900 field-emission scanning electron microscope. Transmission electron microscopy (TEM) was specifically employed to examine the nanostructural features of 13 μm foil. Tensile testing was carried out on 13 μm specimens using a micro-mechanical testing system, with strain rates maintained at 1×10^{-3} s^{-1}, to evaluate mechanical performance parameters including yield strength, ultimate tensile strength, and elongation.

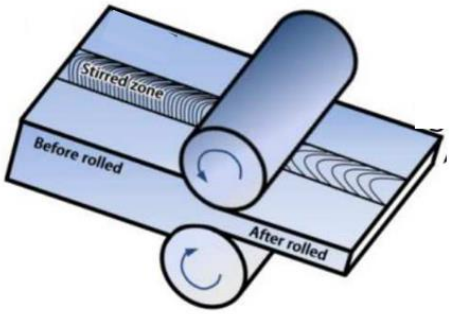

Figure 1 Schematic of rolling process

3. Results and Discussion

3.1 Grain Structure Evolution

The grain structure of the 1100 aluminum alloy 6.8mm cast-rolled plate is shown in Figure 2. The cast-rolled plate samples were characterized using polarized light microscopy after anodic coating. During electrolytic coating, a thin oxide layer forms on the aluminum alloy surface, with its thickness directly related to the applied voltage and electrolysis time. Different grain orientations exhibit varying coating deposition rates during electrolysis, resulting in distinct colors under polarized light due to optical interference.

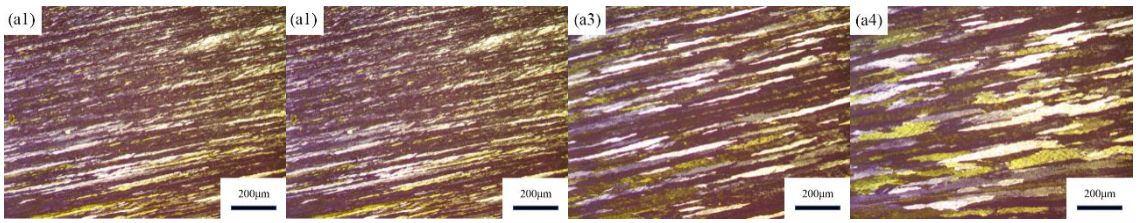

Figure.2 Grain structure of 1100 aluminum alloy cast-rolled plate (a1, a2, a3, a4 correspond to positions at 0 (edge), 1/6, 1/3, and 1/2 thickness from the edge, respectively).

The figure reveals fibrous grains in the cast-rolled plate. Grain size gradually increases from the edge to the center of the plate, with edge grains showing the highest aspect ratio (length-to-width ratio) and mid-thickness (1/2 position) grains having the lowest. The fibrous microstructure distribution is consistent across both alloys studied. The symmetry axis of the cast-rolled grains lies in the center layer of the ND plane, and the columnar grains in both alloys are oriented approximately 15 ° relative to the center layer. These characteristics arise from the rapid solidification during cast rolling. The water-cooled rolls act as crystallizers during melt solidification, causing grains to preferentially grow along the fastest heat dissipation direction. Consequently, the columnar grain axes are perpendicular to the rolling plane.

Due to rapid heat dissipation at the upper and lower surfaces of the cast-rolled blank, higher undercooling at the surfaces promotes elevated nucleation rates and rapid crystallization, forming fine grains. As the solid-liquid interface advances toward the center, the undercooling decreases, slowing crystallization and allowing sufficient time for dendrite growth, which leads to coarser grains in the central layer.

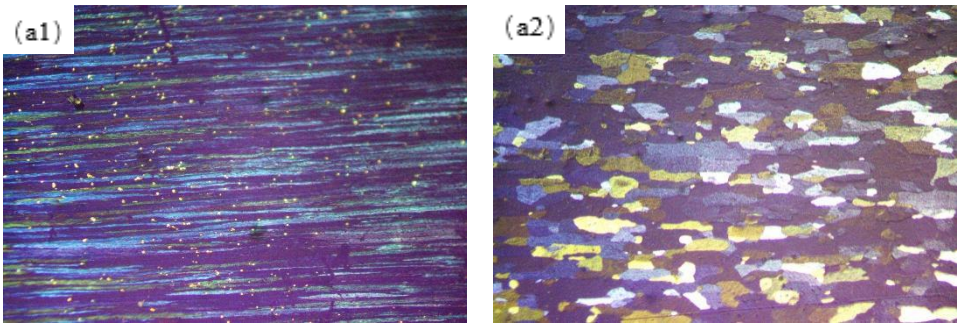

Figure.3 Microstructure of 2.2mm aluminum foil (a1: before annealing; a2: after annealing).

Figure 3 illustrates the metallographic diagrams of the 2.2mm cold-rolled sheet and its annealed counterpart. After rolling deformation, the 1100 aluminum alloy exhibits fibrous grains. Following intermediate annealing at 460 ℃ for 3 hours, the fibrous grains grow and transform into equiaxed grains. The purpose of intermediate annealing is to relieve residual stress and enhance the foil's deformability.

Figure 4 shows the grain morphology of cold-rolled sheets at thicknesses of 0.96mm, 0.42mm, and 0.24mm. During the first rolling pass to 0.96mm (56% reduction), grains elongate along the rolling direction, forming a fibrous structure with dislocation tangles and minor subgrain boundaries. The through-thickness grain dimension decreases to 5–10 μm.

At the 0.42mm stage (total reduction: 81%), grains further flatten, achieving an aspect ratio exceeding 10:1. Dislocation density increases significantly, forming dislocation cell structures, while deformation twins appear in localized regions.

The final 0.24mm sheet (total reduction: 89%) exhibits a highly aligned fibrous microstructure, with grains compressed to 1–3 μm in thickness. Numerous shear bands and deformation bands develop internally, and subgrain sizes refine to submicron-scale. The entire process is dominated by work-hardening mechanisms without dynamic recrystallization, resulting in pronounced anisotropic characteristics.

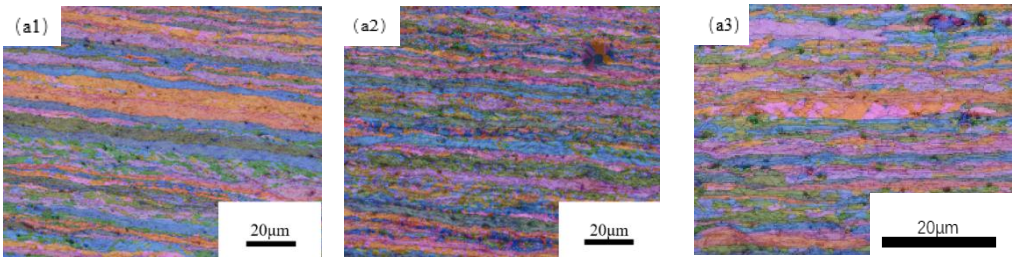

Figure.4 Grain structure of cold-rolled 1100 aluminum alloy (a1: 0.96 mm, a2: 0.42 mm, a3: 0.24 mm).

Figure 5 illustrates the grain morphology of aluminum foils at thicknesses of 0.1mm, 40μm, and 13μm, revealing superplastic deformation and nanoscale structural evolution during extreme thinning. At 0.1mm thickness, the original fibrous grains are compressed to 200–500nm in thickness, forming lamellar nanocrystalline bands parallel to the rolling direction. Grain boundaries become blurred with abundant cubic texture components, and subgrain sizes refine to 50–80nm.

Upon further rolling to 40μm, grain thickness sharply decreases to 80–150nm, exhibiting wavy or serrated grain boundaries. Dislocation cell structures collapse into continuously distributed dislocation walls, while discontinuous dynamic recovery generates equiaxed nanograin nuclei in localized regions.

At the critical thickness of 13μm, grains evolve into highly elongated nanofibrous bundles (1–2μm in length, 20–50nm in width) with aspect ratios exceeding 40:1. Fragmented equiaxed grains are also observed due to grain crushing. Grain boundaries remain indistinct and adopt zigzag arrangements, while internal lamellar substructures become densely packed. Shear bands develop periodic nanoscale striations (spacing ~200nm) embedded with equiaxed nanograins (10–15nm). The overall microstructure demonstrates strong directional alignment along the rolling axis, accompanied by ultrafine fragments from grain fracture and wavy grain boundary contours, reflecting intense plastic flow under extreme rolling conditions.

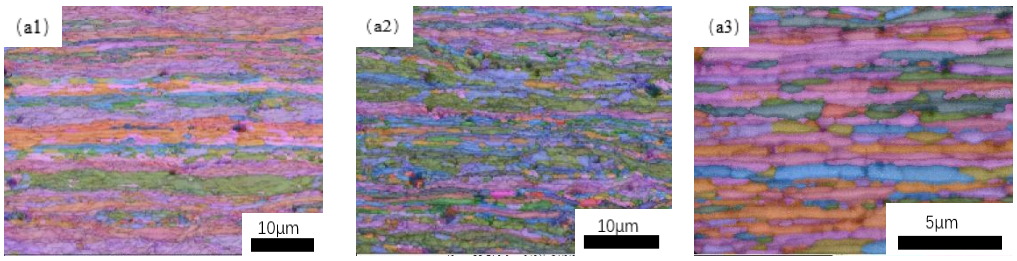

Figure.5 Grain structure of cold-rolled 1100 aluminum alloy (a1: 0.1 mm, a2: 40 μm, a3: 13 μm).

3.2 TEM micrograph of 13μm aluminum foil

Figure 6 presents the TEM micrograph of 13μm aluminum foil subjected to severe plastic deformation. The transmission results reveal a high density of dislocations, with clearly visible dislocation tangles and walls. These defects arise from the extreme plastic deformation that significantly elongates and flattens internal grains, creating non-uniform strain distribution and localized stress concentration.

Subgrains are also observed, formed by the rearrangement of dislocations introduced during heavy cold rolling. These subgrains nucleate through dislocation clustering and subsequently grow by absorbing surrounding dislocations. Analysis of the dislocation network indicates distinct grain

encapsulation phenomena, particularly in regions with grain sizes around 800nm, where pronounced dislocation pile-ups occur near grain boundaries.

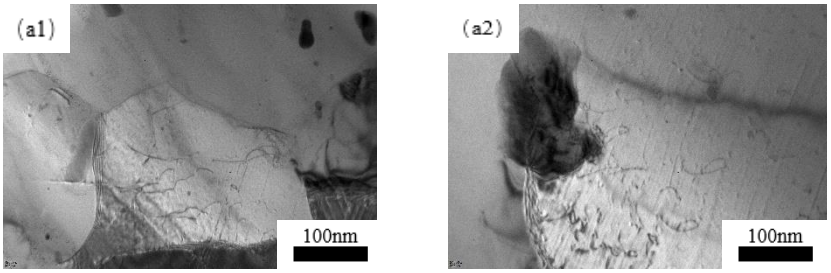

Figure.6 TEM Image of 13μm Aluminum Foil

This spatial distribution of dislocations originates from the strong obstruction of dislocation motion by grain boundaries during plastic deformation. The dense entanglement of dislocations near boundaries and their mutual interactions substantially increase resistance to dislocation glide. Macroscopically, this mechanism manifests as simultaneous enhancement of tensile strength and elongation. The continuous accumulation of internal stresses during deformation necessitates higher external loads to overcome intense dislocation interactions, thereby improving both strength (250MPa) and ductility (3.5%).

3.3 Mechanical Properties Analysis of 13μm Aluminum Foil

As a high-end aluminum foil product, the whole production process of battery foil has strict control, especially for the process adaptability requirements of lithium-ion battery aluminum foil coating and rolling and cell assembly, the core process parameters must be strictly standardized, such as strict technical requirements in melt quality, flatness, thickness uniformity and surface quality. The stability of mechanical properties directly affects the production efficiency. When the tensile strength and ductility are not up to standard, the risk of belt breakage will be significantly increased. The performance requirements for the 13 μ m thick aluminum foil of series 1 battery are: the mechanical properties should meet the hardness index of tensile strength ≥ 180MPa and elongation ≥ 2%, and the surface quality requirement is zero pinhole. Tensile test was carried out on 1100 finished aluminum foil, and the average value was obtained after three times of tensile test for each sample. The results showed that the tensile strength was 250Mpa; The elongation is 3.5.

As a typical non-heat-treatable strengthened alloy, 1xxx-series aluminum alloys rely solely on three strengthening mechanisms after rolling deformation: grain refinement strengthening, dislocation strengthening, and second-phase strengthening. Among these, grain refinement strengthening stands as one of the most widely utilized methods for simultaneously enhancing strength and toughness in metallic materials.

3.3.1 Grain refinement strengthening

The finer the grains, the greater the grain boundary area per unit volume, which increases resistance to dislocation motion and thus enhances alloy strength. For wrought aluminum alloys, three methods are used to refine grains: (1) refining as-cast grains; (2) controlling dispersed phases to refine recrystallized grains; (3) applying deformation and recrystallization to refine recrystallized grains. These methods are often used in combination. The contribution of grain refinement strengthening can be calculated using the Hall-Petch formula[6]:

$$\Delta\sigma_{gb}=Kd_R^{-1/2} \quad (1)$$

In the formula, K represents the Hall-Petch slope, whose value depends on the material type. For 1xxx-series aluminum alloys (e.g., industrial-purity grades like 1060 and 1100), the K value ranges from 0.07 to 0.15 MPa $m^{1/2}$. dR denotes the average grain size. After over 99% deformation, the aluminum foil develops exceptionally fine grains. Consequently, the high strength-toughness and formability of the 13μm 1100 aluminum foil primarily depend on the grain refinement strengthening mechanism.

3.3.2 Second-phase strengthening

Figure 7 shows the second-phase particle distribution in 13μm aluminum foil. The image reveals a high density of large-volume second-phase particles. When dislocations interact with these particles, two distinct mechanisms occur:1)Dislocation cutting through second-phase particles: When dislocations encounter softer second-phase particles, they may cut through them, causing the particles to move with the matrix. This process leaves a step at the particle-matrix interface with a height equal to the Burgers vector. Cutting requires additional energy expenditure, enhancing strength by dissipating deformation energy.2)Dislocation bypassing second-phase particles: When dislocations cannot cut through hard particles, they bypass them, leaving dislocation loops around the particles. The critical shear stress required for bypassing is given by the equation below:

$$\tau = \frac{Gb}{\lambda} \tag{2}$$

where τ is the shear stress, G is the shear modulus, and b is the Burgers vector. This strengthening effect is related to the spacing of second-phase particles—the smaller the interparticle spacing, the more pronounced the strengthening effect.

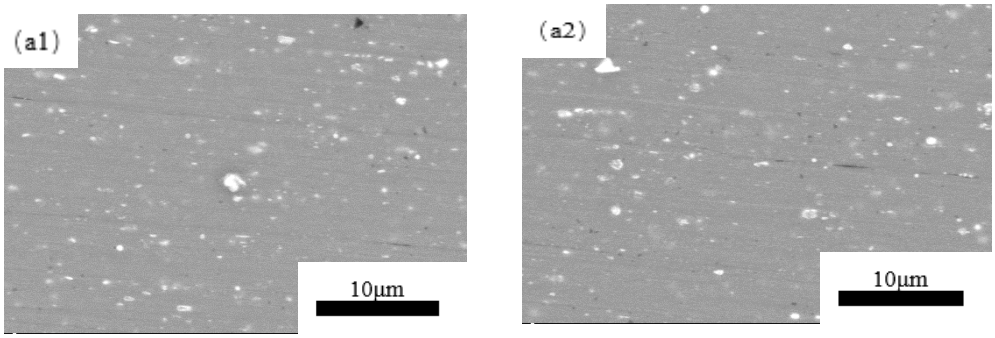

Figure.7 TEM Image of 13μm Aluminum Foil

3.3.2 Dislocation strengthening

Dislocation strengthening is a critical mechanism in metallic materials that enhances strength by increasing dislocation density. The fundamental principle lies in the proliferation, motion, and mutual obstruction of dislocations during plastic deformation, which significantly raises the material's internal deformation resistance. When external forces act on the material, dislocations glide along slip planes, causing plastic deformation. As deformation progresses, dislocations interact with other dislocations, grain boundaries, or second-phase particles, forming complex structures such as dislocation tangles, walls, or cells. These structures act as pinning points that impede further dislocation motion, requiring subsequent dislocations to overcome higher stresses via mechanisms like cross-slip or climb, thereby increasing the material's yield strength. In wrought aluminum alloys, the relationship between dislocation-induced strength (Δσd) and dislocation density (ρ) can be described by the Taylor equation[7]:

$$\Delta\sigma_d = M\alpha Gb\sqrt{\rho} \quad (3)$$

where M=3.06 is the Taylor factor[8], α=0.3 is a dimensionless constant[9], G=27 GPa is the shear modulus of pure aluminum, and b=0.286 nm represents the Burgers vector of dislocations in the aluminum alloy[10].

The high dislocation density in 13μm aluminum foil primarily originates from extreme rolling deformation. As the thickness is reduced from millimeter-scale to micrometer-scale, the material undergoes dozens of passes of severe plastic deformation. Each rolling pass generates a substantial number of new dislocations through slip and shear mechanisms. Due to aluminum's high stacking fault energy, dislocations cannot be rapidly eliminated via dynamic recovery processes (e.g., climb or annihilation), leading to continuous dislocation accumulation.

Concurrently, nanoscale grains (20–50 nm) severely restrict dislocation mobility, forcing dislocations to pile up at grain boundaries and form densely tangled structures. Localized superplastic deformation within shear bands further exacerbates dislocation proliferation, ultimately resulting in honeycomb-like dislocation walls and three-dimensional networks. These configurations drive the dislocation density beyond conventional limits, serving as the primary source of the material's ultrahigh strength.

4. Conclusion

1) Evolution law of grain structure

The grain shape of 1100 aluminum alloy changed regularly in different processing stages: at the initial casting, the grain was like a slender fiber (similar to elongated rice grain), and the central grain was thicker than the edge; During the cold rolling process, the grains are flattened and stretched, and the thickness is compressed from millimeter level to nanometer level, with a large number of micro defects inside; During high temperature annealing, the grains will recrystallize and grow up. In the subsequent rolling process, the grains will become more and more fibrotic, and some small equiaxed grains will appear in the finished aluminum foil.

2) Microstructure (TEM) of 13μm Aluminum Foil

The 13μm-thick 1100 aluminum foil exhibits a complex microstructure dominated by severe dislocation tangles and walls, resulting from extreme rolling-induced grain elongation and flattening. The heavy deformation creates a composite nanostructure comprising nanoscale grains (20–50 nm) and ultrahigh dislocation density ($>10^{15}$ m^{-2}). Through synergistic interactions of "micro-obstacles" (dislocation walls, grain boundaries, and subgrains), this architecture achieves a balance between high strength (250 MPa tensile strength) and processability. TEM characterization reveals lamellar nanocrystalline bands, periodic nanoscale striations (spacing ~200 nm), and dense dislocation networks. Pronounced dislocation pile-ups at grain boundaries severely restrict dislocation mobility, requiring elevated external stresses to drive plastic deformation. While enhancing strength, dynamic dislocation rearrangement maintains plasticity (3.5% elongation), ultimately meeting the stringent requirements for battery foil applications—high strength, fracture resistance, and processing stability under high-speed coating/rolling conditions.

3) Strengthening Mechanisms of Aluminum Foil

The 13μm aluminum foil achieves exceptional mechanical properties (tensile strength: 250 MPa, elongation: 3.5%) through severe rolling deformation, exceeding battery foil specifications (required: tensile strength ≥180 MPa, elongation ≥2%). This performance originates from multi-mechanism collaborative strengthening: 1) Grain refinement strengthening – nanoscale grains (20-50 nm) impede dislocation motion via grain boundary blocking; 2) Dislocation strengthening – high-density dislocation tangles, walls, and subgrains significantly elevate deformation resistance; 3) Second-

phase strengthening – hard particles force dislocations to bypass or cut through precipitates, inducing energy dissipation. These synergistic effects fulfill dual requirements for battery foil applications: high fracture resistance and formability during electrode processing.

Acknowledgements

The authors would like to express their gratitude to Prof. Pan for his guidance and support.

References

[1] Hansen N ,Yu B T ,Mishin V O , et al.Coupling of Local Texture and Microstructure Evolution during Restoration Processes in Aluminum Deformed to Large Strains[J].Materials Science Forum,2013,2379(753-753):251-256.
[2] Qing-lin D ,Chang L ,Xiao-hui C , et al.Fabrication of ultrafine-grained AA1060 sheets via accumulative roll bonding with subsequent cryorolling[J].Transactions of Nonferrous Metals Society of China,2021,31(11):3370-3379.
[3] Horita Z ,Ohashi K ,Fujita T , et al.Achieving High Strength and High Ductility in Precipitation-Hardened Alloys[J].Advanced Materials,2005,17(13):1599-1602.
[4] Cheng S , Ma E .Simultaneously Increasing the Ductility and Strength of Nanostructured Alloys[J]. Advanced Materials, 2010, 18(17):2280-2283.DOI:10.1002/adma.200600310.
[5] Cheng S , Zhao Y H , Zhu Y T ,et al.Optimizing the strength and ductility of fine structured 2024 Al alloy by nano-precipitation[J].Acta Materialia, 2007, 55(17):5822-5832. DOI:10.1016/j.actamat.2007.06.043.
[6] Pande C S, Cooper K P. Nanomechanics of Hall–Petch relationship in nanocrystalline materials. Progress in Materials Science, 2009,54(6):689-706.
[7] Hsu C J, Chang C Y, Kao P W, et al. Al–Al3Ti nanocomposites produced in situ by friction stir processing. Acta Materialia, 2006,54(19):5241-5249.
[8] Stoller R E, Zinkle S J. On the relationship between uniaxial yield strength and resolved shear stress in polycrystalline materials[J]. Journal of nuclear materials, 2000,283-287: 349-352.
[9] Ashby M F. The deformation of plastically non-homogeneous materials[J]. Philosophical magazine (London, England : 1945), 1970,21(170): 399-424.
[10] Ma K, Hu T, Yang H, et al. Coupling of dislocations and precipitates: Impact on the mechanical behavior of ultrafine grained Al–Zn–Mg alloys[J]. Acta Materialia, 2016,103: 153-164.